



# Effect of heating time on bonding interface, atom diffusion and mechanical properties of dissimilar titanium joints produced by thermal self-compressing bonding

Yun-hua DENG<sup>1</sup>, Qiao GUAN<sup>1,2</sup>, Jun TAO<sup>1</sup>

1. Aeronautical Key Laboratory for Welding and Joining Technologies,

AVIC Beijing Aeronautical Manufacturing Technology Research Institute, Beijing 100024, China;

2. School of Mechanical Engineering and Automation, Beihang University, Beijing 100191, China

Received 5 November 2016; accepted 22 May 2017

**Abstract:** Solid-state bonding between pure titanium and Ti6Al4V (TC4) alloy was conducted by a new bonding method named as rigid restraint thermal self-compressing bonding. Effects of heating time on bonding interface, atom diffusion and mechanical properties of the joints were studied. Results show that atom diffusion between pure titanium and TC4 alloy significantly takes place during bonding. The diffusion depths of Al and V in pure titanium side are increased with increasing heating time. Due to the enhancement of atom diffusion, bond quality of the bonding interface is improved along with the increase of heating time. The heating time seems to have little effect on microhardness distribution across the joint. However, the tensile strength and ductility of the joint have close relation to heating time. Prolonging heating time can improve the tensile strength and ductility of the joint, especially the latter. When the heating time increases to 450 s, solid-state joint with good combination of strength and ductility is attained.

**Key words:** dissimilar titanium alloys joining; rigid restraint thermal self-compressing bonding; atom diffusion, mechanical properties

## 1 Introduction

To satisfy the increasingly strict requirements of excellent performance, long life, high reliability, high security and so on, advanced structural materials with perfect mechanical and physical properties have been developed for both civil and military aircraft. With distinguished advantages of lower density, high specific strength, high specific stiffness and good resistance to corrosion and heat, titanium and its alloy are one kind of these main structural materials, and they have played an increasingly significant role in the aviation industry [1–4]. Welding process is an indispensable technique for manufacturing titanium components, and a variety of welding methods have been developed to join titanium, such as electron beam (EB) welding [5,6], laser beam (LB) welding [7,8], brazing [9,10], diffusion bonding [11,12] and friction welding [13,14]. Among these methods, solid-state bonding method has drawn particular attention as it can avoid the solidification

problems occurred in fusion processes and produces sound solid-state joint with better combination of strength and ductility.

Rigid restraint thermal self-compressing bonding (TSCB) is a new solid-state bonding process. During the process, a local non-melted heating method is employed to heat the butt interface of rigid restrained plates to be bonded as illustrated in Fig. 1 [15]. Under the action of localized scanning heating of EB, LB or other types of heat source, materials close to the butt interface are expanded. Due to the existence of surrounding cool metals and rigid restraints, the expansion of high temperature materials is restrained; and thus a compressive pressure ( $p$ ) is developed which compresses the high temperature metals near the bonding interface and facilitates the atom diffusion between butt-weld specimens to produce permanent solid-state joint. Utilizing the localized stress–strain field to accomplish atom bonding between butt-weld specimens, rigid restraint TSCB can avoid the use of external force. Previous study has proved the feasibility of rigid restraint

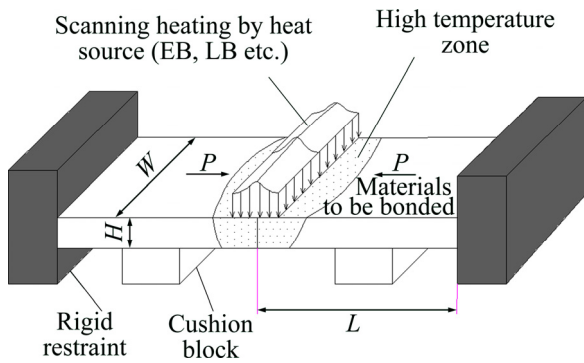


**Fig. 1** Illustration of rigid restraint TSCB

TSCB to join titanium alloy [15]. However, the atom diffusion behavior during bonding was not studied because the similar materials were chosen in previous work.

In this study, pure titanium and Ti6Al4V alloy were bonded together at different heating time. The bonding interfaces and the concentration profiles of Ti, Al and V across the bonding interfaces at different heating time were analyzed to study the atom migration and the effect of heating time on the atom migration during rigid restraint TSCB. At the same time, microhardness distributions and tensile mechanical properties of joints at different heating time were determined to analyze the effect of heating time on the mechanical properties of joints.

## 2 Experimental

### 2.1 Materials

Pure titanium and Ti6Al4V alloy with the dimensions of 59 mm ( $L$ )  $\times$  50 mm ( $W$ )  $\times$  5 mm ( $H$ ) were used in this work. The nominal chemical compositions of pure titanium and Ti6Al4V alloy are listed in Table 1. It can be seen that Ti6Al4V alloy has 5.5%–6.8% of the  $\alpha$  stabilizing element Al, 3.5%–4.5% of the  $\beta$  stabilizing element V, and about 90% of Ti element, while pure titanium only has Ti but no Al and V elements. This notable chemical compositions difference paves the way for investigating the atom diffusion during rigid restraint TSCB.

**Table 1** Nominal chemical compositions of pure titanium and Ti6Al4V alloy (mass fraction, %) [16]

| Sample        | Al      | V       | Fe         | C          | N           | H            | O           | Ti   |
|---------------|---------|---------|------------|------------|-------------|--------------|-------------|------|
| Pure titanium | 0       | 0       | $\leq 0.3$ | $\leq 0.1$ | $\leq 0.05$ | $\leq 0.015$ | $\leq 0.25$ | Bal. |
| Ti6Al4V alloy | 5.5–6.8 | 3.5–4.5 | $\leq 0.3$ | $\leq 0.1$ | $\leq 0.05$ | $\leq 0.015$ | $\leq 0.2$  | Bal. |

### 2.2 Rigid restraint TSCB between Ti6Al4V and pure titanium

Pure titanium and Ti6Al4V plates to be bonded were cleaned with acid solution and swabbed with ethanol. Electron beam was employed as the heat source. Rigid restraint TSCB between pure titanium and Ti6Al4V alloy was carried out in a high voltage vacuum electron beam welding machine ZD150-15MH CV3M. Multi-beam scanning heating method controlled by electron beam deflection system was employed to heat the butt interfaces. Scanning length and scanning frequency were selected as 50 mm and 100 Hz, respectively. Other experimental parameters are shown in Table 2.

**Table 2** Parameters of rigid restraint TSCB of pure titanium to Ti6Al4V alloy

| Beam voltage/kV | Focus current/mA | Beam current/mA | Heating time/s |
|-----------------|------------------|-----------------|----------------|
| 150             | 2809             | 1.8             | 210            |
|                 |                  |                 | 270            |
|                 |                  |                 | 330            |
|                 |                  |                 | 450            |

### 2.3 Analysis of joints

After bonding, specimens used for metallographic analysis were machined transversely through the bonding interface and mounted in bakelite for grinding and polishing. The polished cross-sections after etching were characterized by a Leica DM6000M optical microscope (OM). A Quanta 250FEG scanning electron microscope (SEM) with energy dispersive spectrometer (EDS) was employed to analyze the element concentration profiles across the bonding interface. The bond quality was assessed on the basis of residual voids at the bonding interface.

Microhardness and tensile mechanical properties of present dissimilar joints with heating time of 210 and 450 s were tested. A hardness tester (HXD1000) was used to test the microhardness of joints at room temperature under a test load of 300 g for 10 s. Three tensile specimens perpendicular to the bonding interface for present dissimilar joints and base metals were machined. The Quanta 250FEG SEM was employed to analyze the morphology characteristics of the fractured surfaces of the tensile test specimens.

## 3 Results and discussion

### 3.1 Bonding interface of joints

Optical microscope graphs of the bonding interfaces with different heating time are presented in Fig. 2. At the heating time of 210 s, many voids distributed at the

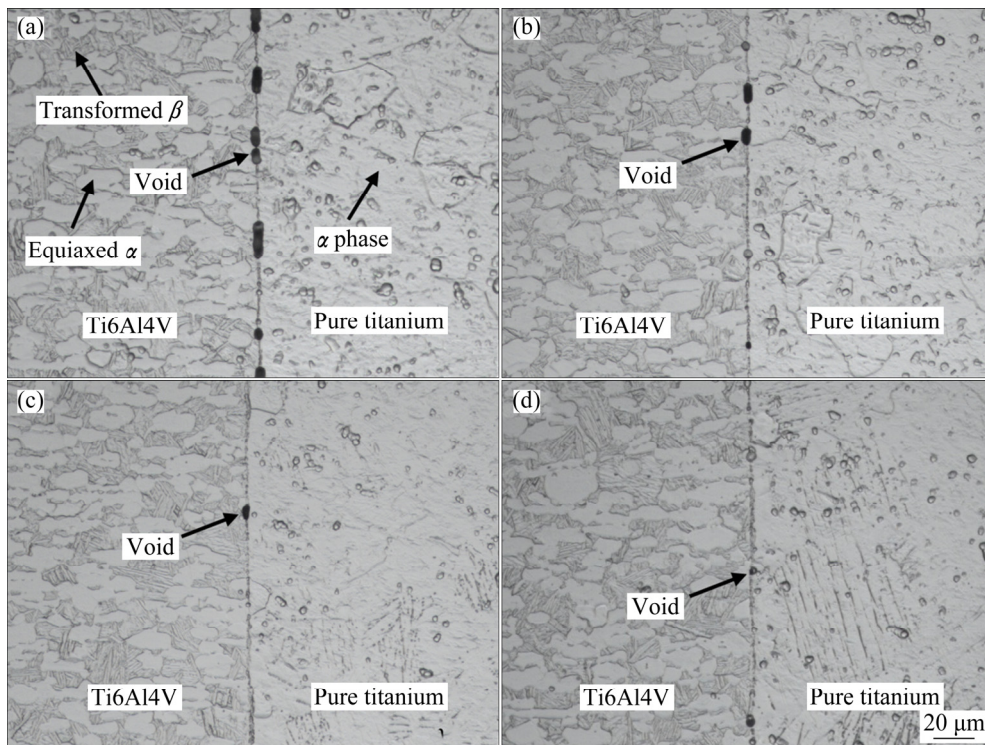


Fig. 2 OM graphs of bonding interfaces produced at different heating time: (a) 210 s; (b) 270 s; (c) 330 s; (d) 450 s

bonding interface can be observed and the length of single void can approach to  $10\ \mu\text{m}$  as shown in Fig. 2(a), which indicates that the bond quality is not satisfied. As the heating time increases to 270 s, the number of residual voids decreases and the size of the voids is also smaller than that of joint bonded at the heating time of 210 s. At 330 s, as shown in Fig. 2(c), the number and size of voids are further diminished compared with those of the joint at 270 s. There are only few small voids at the bonding interface, when the heating time increases to 450 s, as presented in Fig. 2(d). Therefore, it can be concluded that heating time has notable effect on the bond quality of the interfaces. With the increase of heating time, the number and size of voids are decreased and the bond quality is improved accordingly.

Although rigid restraint TSCB has much difference compared with diffusion bonding, it still relies on atom diffusion to produce solid-state joint with sound bonding interface and good bond strength. With the increase of heating time, the dwell time over high temperature and the volume of the materials with high temperature are increased, which facilitates the atom diffusion between pure titanium and Ti6Al4V alloy. Moreover, during rigid restraint TSCB, an internal elasto-plastic stress-strain field is developed by localized heating according to the numerical analysis of Ref. [17]. With the increase of heating time, the plastic deformation at bond interface is increased due to the prolonged time of materials subjected to thermal compressive action produced by the

internal elasto-plastic stress-strain field. Plastic deformation also enhances the atom diffusion across bonding interface as shown in Ref. [18]. Therefore, improved bond quality between pure titanium and Ti6Al4V alloy is attained with the increase of heating time.

### 3.2 Element profiles across bonding interface

As shown in Fig. 2(a), the microstructure of Ti6Al4V alloy is made up of equiaxed  $\alpha$  phase and transformed  $\beta$  phase while only  $\alpha$  phase is contained in pure titanium. Therefore, two kinds of bond regions exist around the bonding interfaces of present dissimilar joints. One is  $\alpha_{\text{Ti6Al4V}}/\alpha_{\text{pure-titanium}}$  region, where the equiaxed  $\alpha$  of Ti6Al4V alloy and the  $\alpha$  phase of pure titanium are bonded together, and the other is  $\beta_{\text{Ti6Al4V}}/\alpha_{\text{pure-titanium}}$  region which is composed of transformed  $\beta$  of Ti6Al4V alloy and the  $\alpha$  phase of pure titanium. Element concentration profiles of Ti, Al and V across the bonding interface in  $\alpha_{\text{Ti6Al4V}}/\alpha_{\text{pure-titanium}}$  zone obtained from EDS analysis are shown in Fig. 3.

At the heating time of 210 s, it can be seen clearly that Al and V migrate into pure titanium and both contents are decreased with increasing the distance away from the bonding interface in pure titanium substrate. The concentrations of Al and V equal to zero at about  $1.5\ \mu\text{m}$  away from the bonding interface in the pure titanium side. Conversely, the titanium profile shows an upward trend from the Ti6Al4V to pure titanium side as

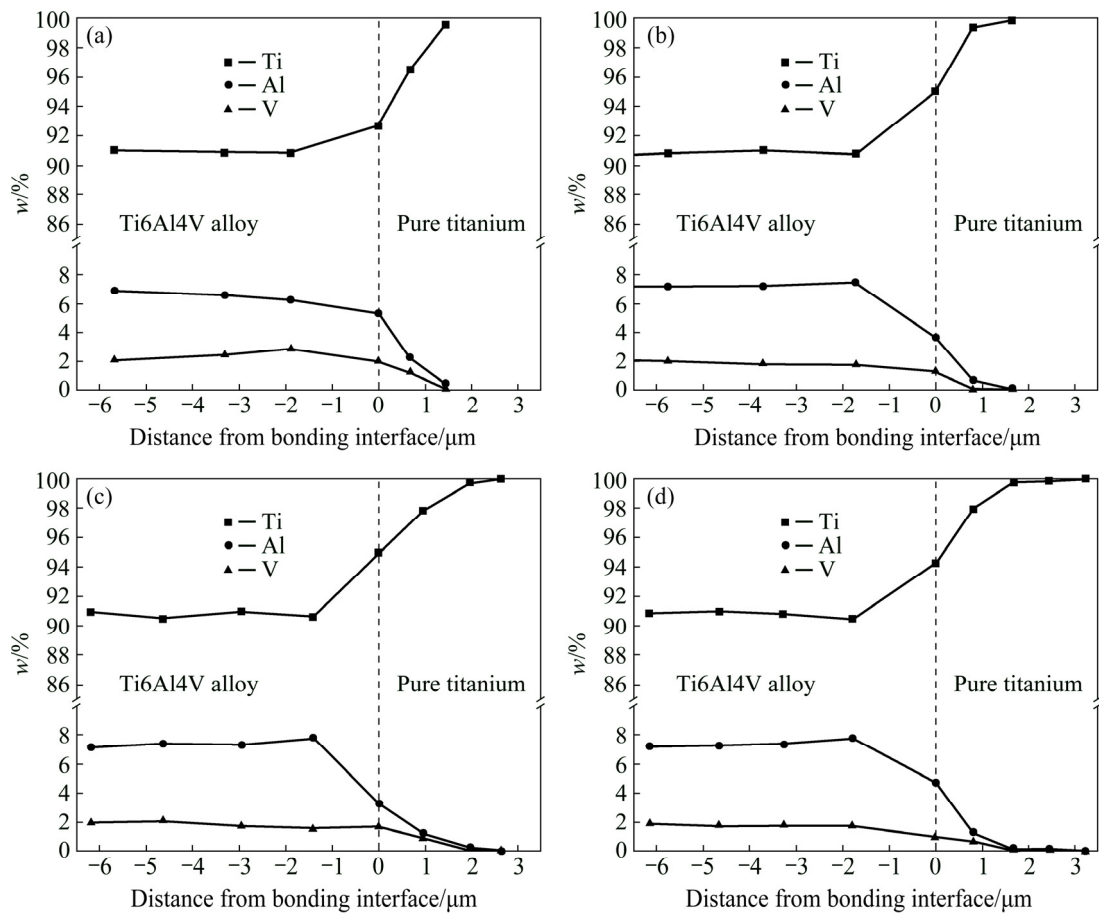


**Fig. 3** Concentration profiles across bonding interface in  $\alpha_{\text{Ti6Al4V}}/\alpha_{\text{pure-titanium}}$  zone at different heating time: (a) 210 s; (b) 270 s; (c) 330 s; (d) 450 s

the content of Ti in pure titanium substrate is higher than that in Ti6Al4V substrate.

At the heating time of 270, 330 and 450 s, the similar concentration profiles of Ti, Al and V in  $\alpha_{\text{Ti6Al4V}}/\alpha_{\text{pure-titanium}}$  zone can be seen from Fig. 3. Moreover, it can be seen that with the increase of heating time, the diffusion depths of Al and V in pure titanium side are increased, reaching appropriately 2.5–3.0  $\mu\text{m}$  away from the bonding interface at the heating time of 450 s, because of the improved atom diffusion along with the increase of heat time.

Element concentration profiles across the bonding interface in  $\beta_{\text{Ti6Al4V}}/\alpha_{\text{pure-titanium}}$  zone are shown in Fig. 4.

It can be seen that concentrations of Ti, Al and V in  $\beta_{\text{Ti6Al4V}}/\alpha_{\text{pure-titanium}}$  region display similar diffusion behavior as those in  $\alpha_{\text{Ti6Al4V}}/\alpha_{\text{pure-titanium}}$  region, but the diffusion depths of Al and V in  $\beta_{\text{Ti6Al4V}}/\alpha_{\text{pure-titanium}}$  region are larger compared with  $\alpha_{\text{Ti6Al4V}}/\alpha_{\text{pure-titanium}}$  region at the same heating time. Taking the diffusion depth at the heating time of 450 s for example, the diffusion depth is 2.5–3.0  $\mu\text{m}$  in  $\alpha_{\text{Ti6Al4V}}/\alpha_{\text{pure-titanium}}$  region whilst it is approximately 4.0  $\mu\text{m}$  in  $\beta_{\text{Ti6Al4V}}/\alpha_{\text{pure-titanium}}$  region.

Previous studies confirmed that the diffusion coefficient of atom in  $\beta$  phase is larger than that in  $\alpha$

phase [19]. Therefore, atoms in  $\beta_{\text{Ti6Al4V}}/\alpha_{\text{pure-titanium}}$  zone diffuse farther than those in  $\alpha_{\text{Ti6Al4V}}/\alpha_{\text{pure-titanium}}$  zone according to the relation among the diffusion distance ( $x$ ), the diffusion coefficient ( $D$ ), and diffusion time ( $t$ ) [19].

$$x = \sqrt{Dt} \quad (1)$$

### 3.3 Mechanical properties

#### 3.3.1 Microhardness profiles

Microhardness distributions across the bonding interfaces of the dissimilar solid-state joints between pure titanium and Ti6Al4V titanium alloy were tested in this work and the results are illustrated in Fig. 5. When the heating time is 210 s, it can be seen that the microhardness in the Ti6Al4V side fluctuates in the interval of HV (328±11) which is much higher than that in the pure titanium side, whereas the microhardness at the bonding interface is between them. When the heating time increases to 450 s, similar microhardness profile is obtained as shown in Fig. 5(b). Therefore, it can be concluded that the microhardness distribution seems not to be influenced by heating time. The reason concerning with the microstructure was not changed significantly with the change of heating time as shown in Fig. 2.

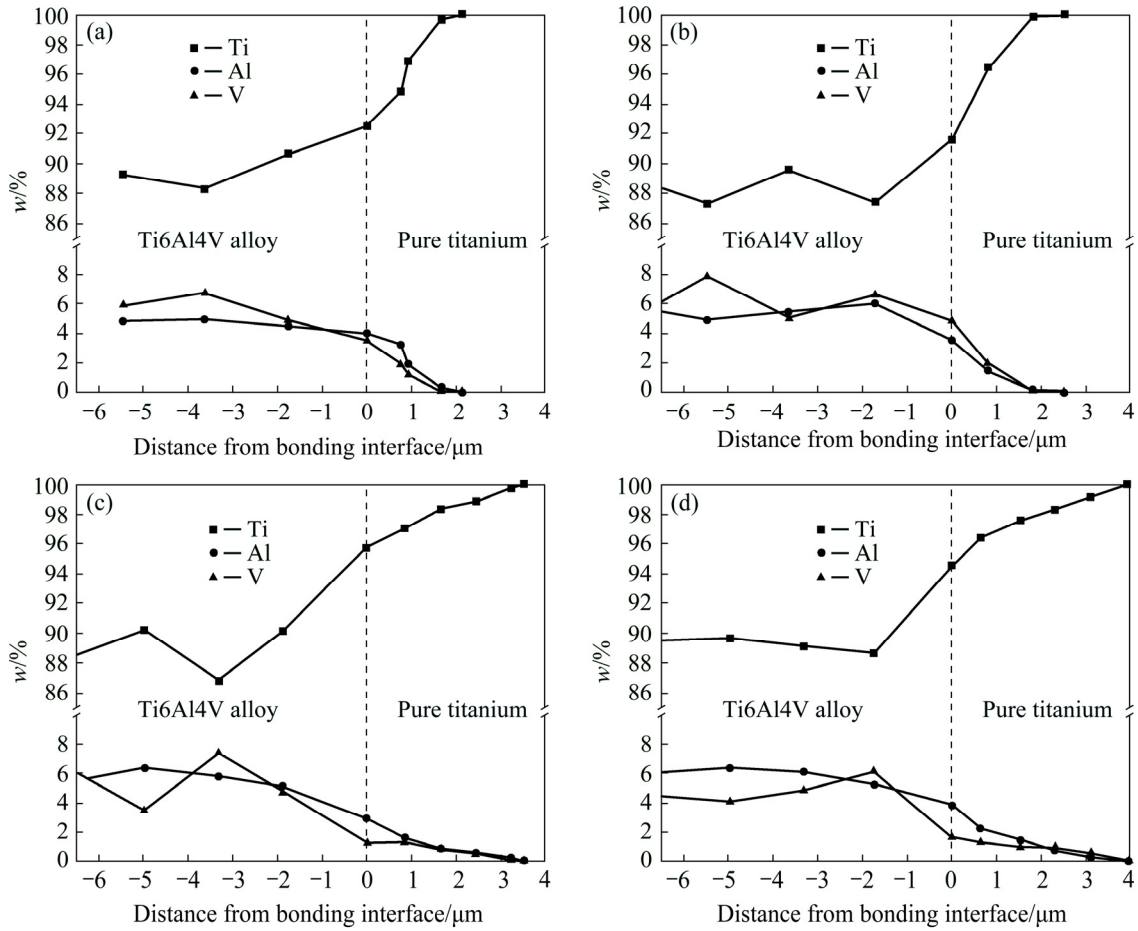


**Fig. 4** Concentration profiles across bonding interface in  $\beta_{\text{Ti6Al4V}}/\alpha_{\text{pure-titanium}}$  zone at different heating time: (a) 210 s; (b) 270 s; (c) 330 s; (d) 450 s

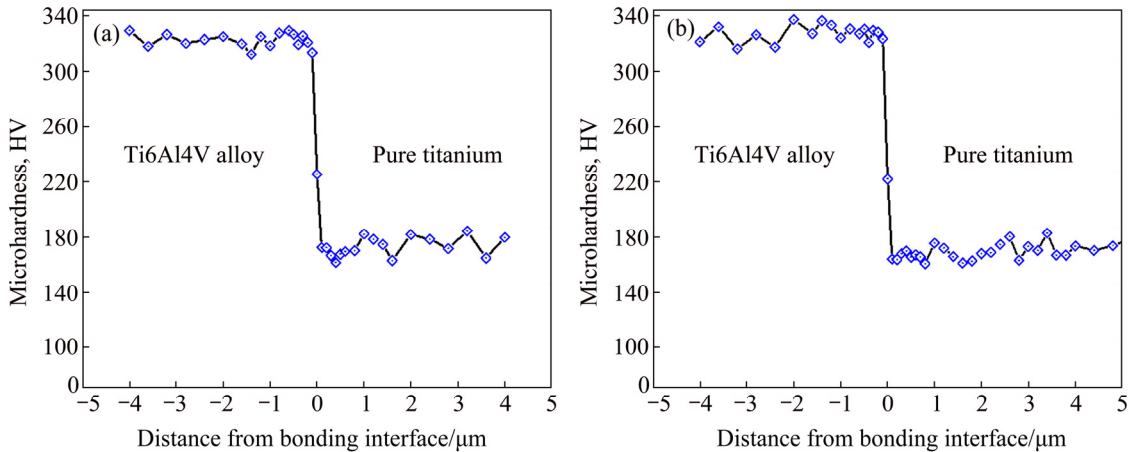


**Fig. 5** Microhardness profiles across bonding interfaces at different heating time: (a) 210 s; (b) 450 s

3.3.2 Tensile mechanical properties

Tensile test results of the joint and base metals are shown in Table 3. It can be seen that compared with the mechanical properties of pure titanium, Ti6Al4V titanium alloy has higher strength but lower elongation, which is related to the additive elements of Al and V in Ti6Al4V alloy.

At the heating time of 210 s, the tensile strength of the joint is 437.4 MPa which is slightly lower than that of pure titanium but the elongation is 0 approximately. Fracture locations of the tensile specimens are located at the bonding interface of the joint as presented in the bottom left corner of Fig. 6(a), and the fracture surface belonging to pure titanium side of present tensile

specimen was examined by SEM. Overall morphology of the fracture surface appears to be smooth as shown in Fig. 6(a). Further observation of the fracture surface at higher magnification was conducted. As shown in Fig. 6(b), groove zone can be founded. Only Ti element is found in groove zone after the EDS analysis, which suggests that the groove zone is the unbounded defect.

**Table 3** Results of tensile test of joint and base metals of pure titanium and Ti6Al4V alloy

| Sample         | Average tensile strength/MPa | Average yield strength/MPa | Average elongation/% |
|----------------|------------------------------|----------------------------|----------------------|
| Pure titanium  | 479.6                        | 348.7                      | 37.3                 |
| Ti6Al4V        | 999.3                        | 944.7                      | 17.4                 |
| Joint at 210 s | 437.4                        | –                          | ≈0                   |
| Joint at 450 s | 472.5                        | 400.1                      | 32.9                 |

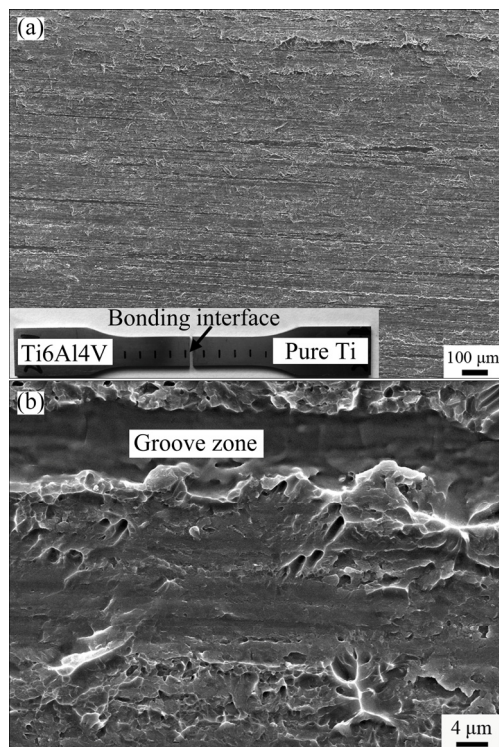


**Fig. 6** Morphologies of tensile fracture surface at heating time of 210 s under lower (a) and higher (b) magnification

When the heating time prolongs to 450 s, the tensile strength and elongation of the joint are increased to 472.5 MPa and 32.9%, respectively. Both of them are close to those of pure titanium, which indicates that the joint has better combination of strength and ductility. The fracture locations of present tensile specimens are located at the pure titanium side as shown in the bottom left corner of Fig. 7, and the fracture morphology of the tensile specimens is shown in Fig. 7. Sound solid-state dissimilar joint with good mechanical properties is attained.

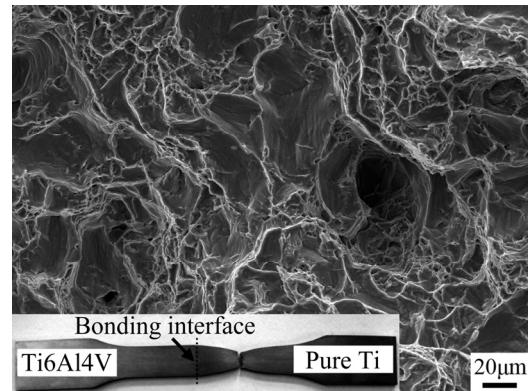


**Fig. 7** Morphology of tensile fracture surface at heating time of 450 s

Therefore, it can be concluded that although the microhardness distribution seems not to be influenced by heating time, the tensile strength and ductility of the joint have close relation to the heating time. With the increase of heating time, the tensile strength and ductility of the joint are increased due to the increase of bond quality. Especially, the ductility of the joint is improved notably.

## 4 Conclusions

1) Pure titanium was bonded to Ti6Al4V alloy by a new solid-state bonding method named as rigid restraint thermal self-compressing bonding which can avoid the use of external forces required in other solid-state bonding methods.

2) Increasing the heating time, the dwell time over high temperature, the volume of materials with high temperature and the plastic deformation at bonding interface are increased which promote the atom diffusion between pure titanium and Ti6Al4V alloy, and thus the number and size of voids at the bonding interface are decreased. When the heating time increases to 450 s, only few small voids retain at the bonding interface.

3) Al and V migrate into pure titanium side and both contents are decreased with increasing the distance away from the bonding interface in pure titanium substrate. Conversely, the titanium profile shows an upward trend from the Ti6Al4V to pure titanium side. The diffusion depths of Al and V in pure titanium side are increased along with the increase of heating time.

4) The microhardness distribution seems not to be influenced by heating time, but the tensile strength and ductility of TSCB joint have close relation to the heating time. With the increase of heating time, the tensile strength and ductility of TSCB joint are increased. Especially, the ductility of the joint has notable improvement.

## Acknowledgements

The authors would like to gratefully acknowledge the financial support provided by Beijing Aeronautical Manufacturing Technology Research Institute and the help provided by Science and Technology, China, on Power Beam Processes Laboratory at Beijing Aeronautical Manufacturing Technology Research Institute, China.

## References

- [1] BOYER R R. An overview on the use of titanium in the aerospace industry [J]. *Materials Science and Engineering A*, 1996, 213(1–2): 103–114.
- [2] WILLIAMS J C, STARKE E A. Progress in structural materials for aerospace systems [J]. *Acta Materialia*, 2003, 51: 5775–5799.
- [3] CUI Chui-xiang, HU Bao-min, ZHAO Li-chen, LIU Shuang-jin. Titanium alloy production technology, market prospects and industry development [J]. *Materials & Design*, 2011, 32: 1684–1691.
- [4] BANERJEE D, WILLIAMS J C. Perspectives on titanium science and technology [J]. *Acta Materialia*, 2013, 61: 844–879.
- [5] ZHANG Bing-gang, SHI Ming-xiao, CHEN Guo-qing, FENG Ji-cai. Microstructure and defect of titanium alloy electron beam deep penetration welded joint [J]. *Transactions of Nonferrous Metals Society of China*, 2012, 22: 2633–2637.
- [6] LU Wei, SHI Yao-wu, LI Xiao-yan, LEI Yong-ping. Effect of electron beam welding on the microstructures and mechanical properties of thick TC4-DT alloy [J]. *Materials & Design*, 2012, 34: 509–515.
- [7] AKMAN E, DEMIR A, CANEL T, SINMAZCELİK T J. Laser welding of Ti6Al4V titanium alloys [J]. *Journal of Materials Processing Technology*, 2009, 209: 3705–3713.
- [8] MA Xu-yi, GONG Shui-li, ZHANG Jian-xun, LU Wei, YANG Jing. Formation, microstructure and mechanical properties of double-sided laser beam welded Ti–6Al–4V T-joint [J]. *Transactions of Nonferrous Metals Society of China*, 2016, 26: 729–735.
- [9] ELREFAEY A, TILLMANN W. Effect of brazing parameters on microstructure and mechanical properties of titanium joints [J]. *Journal of Materials Processing Technology*, 2009, 209: 4842–4849.
- [10] CHUNG T, KIM J, BANG J, RHEE B, NAM D. Microstructures of brazing zone between titanium alloy and stainless steel using various filler metals [J]. *Transactions of Nonferrous Metals Society of China*, 2012, 22: 639–644.
- [11] KURT B, ORHAN N, EVIN E, CALIK A. Diffusion bonding between Ti6Al4V alloy and ferritic stainless steel [J]. *Materials Letters*, 2007, 61: 1747–1750.
- [12] LI Hong, ZHANG Chao, LIU Hong-bin, LI Miao-quan. Bonding interface characteristic and shear strength of diffusion bonded Ti-17 titanium alloy [J]. *Transactions of Nonferrous Metals Society of China*, 2015, 25: 80–87.
- [13] MIRONOV S, ZHANG Y, SATO Y S, KOKAWA H. Crystallography of transformed  $\beta$  microstructure in friction stir welded Ti–6Al–4V alloy [J]. *Scripta Materialia*, 2008, 59: 511–514.
- [14] WELLER M, CHATTERJEE A, HANECZOK G, CLEMENS H. Internal friction of g-TiAl alloys at high temperature [J]. *Journal of Alloys and Compounds*, 2000, 310: 134–138.
- [15] DENG Yun-hua, GUAN Qiao, WU Bing, WANG Xi-chang, TAO Jun. Study on rigid restraint thermal self-compressing bonding—A new solid state bonding method [J]. *Materials Letters*, 2014, 129: 43–45.
- [16] China Aeronautical Materials handbook Edit Committee. *China aeronautical materials handbook* [M]. Beijing: China Standard Publishing Company, 2002. (in Chinese)
- [17] DENG Yun-huang, GUAN Qiao, TAO Jun, WU Bing, WANG Xi-chang. Effect of electron beam power on TC4 alloy rigid restraint thermal self-compressing bonding, microstructure and mechanical properties of joints [J]. *Acta Metallurgica Sinica (Chinese Edition)*, 2015, 51(9): 1111–1120. (in Chinese)
- [18] LI Hong, YANG Chao, SUN Li-xing, Li Miao-quan. Hot press bonding of  $\gamma$ -TiAl and TC17 at a low bonding temperature by imposing plastic deformation and post heating [J]. *Materials Letters*, 2017, 187: 4–6.
- [19] MEHRER H. *Diffusion in solids: Fundamentals, methods, materials, diffusion-controlled process* [M]. Berlin: Springer-Verlag, 2007.

# 加热时间对异种钛合金热自压连接界面、原子扩散和接头力学性能的影响

邓云华<sup>1</sup>, 关桥<sup>1,2</sup>, 陶军<sup>1</sup>

1. 北京航空制造工程研究所 航空焊接与连接技术航空科技重点实验室, 北京 100024;
2. 北京航空航天大学 机械工程及自动化学院, 北京 100191

**摘要:** 采用一种新的固相连接方法——刚性拘束热自压连接方法, 对纯钛和 Ti6Al4V(TC4)钛合金进行固相连接。通过不同加热时间刚性拘束热自压连接界面光学显微镜观察、元素成分能谱分析、显微硬度测试以及接头力学性能测试和断口观察, 分析加热时间对纯钛和 TC4 钛合金异种连接接头界面焊合率、界面元素扩散和力学性能的影响。结果表明: 随着加热时间的增加, 连接界面高温停留时间、高温区材料体积、热挤压应力作用时间增加, 促进界面两侧原子扩散, 界面未焊合缺陷数量和尺寸减少, 焊合质量提高。界面两侧发生显著的元素扩散现象, TC4 合金中 Al 和 V 元素扩散至纯钛中, 纯钛中的 Ti 元素扩散至 TC4 合金中, 并随着加热时间增加, Al 和 V 元素在纯钛中的扩散深度增加。加热时间对接头显微硬度分布影响不显著, 但显著影响接头的强度和塑性, 当加热时间增加至 450 s 时, 可获得综合力学性能较好的纯钛和 TC4 合金异种材料连接接头。

**关键词:** 异种钛合金连接; 刚性拘束热自压连接; 原子扩散; 力学性能

(Edited by Xiang-qun LI)